Vortex line in the unitary Fermi gas

Lucas Madeira, Silvio A. Vitiello, Stefano Gandolfi, and Kevin E. Schmidt

Phys. Rev. A **93**, 043604 — Published 6 April 2016

DOI: 10.1103/PhysRevA.93.043604

A vortex line in the unitary Fermi gas

Lucas Madeira,[1,2,*] Silvio A. Vitiello,[1] Stefano Gandolfi,[3] and Kevin E. Schmidt[2]

[1] *Instituto de Física Gleb Wataghin, Universidade Estadual de Campinas, UNICAMP, Campinas 13083-859, Brazil*
[2] *Department of Physics and Astronomy, Arizona State University, Tempe, Arizona 85287, USA*
[3] *Theoretical Division, Los Alamos National Laboratory, Los Alamos, New Mexico 87545, USA*

We report diffusion Monte Carlo results for the ground state of unpolarized spin-1/2 fermions in a cylindrical container and properties of the system with a vortex line excitation. The density profile of the system with a vortex line presents a non-zero density at the core. We calculate the ground state energy per particle, the superfluid pairing gap and the excitation energy per particle. These simulations can be extended to calculate properties of vortex excitations in other strongly interacting systems, such as superfluid neutron matter using realistic nuclear Hamiltonians.

I. INTRODUCTION

Ultracold Fermi gases are dilute systems with interparticle interactions that can be controlled through Feshbach resonances, which allow the access of strongly interacting regimes. Until recently, superfluids were classified as either Bardeen-Cooper-Schrieffer (BCS) states or the Bose-Einstein Condensate (BEC). In fact they are limit cases of a continuum of the interaction strength. The possibility of tuning the parameters to observe changes from one regime to the other is conceptually interesting, but real enthusiasm came from the experimental realization of the BCS-BEC crossover [1].

The three dimensional unitary Fermi gas is a strongly interacting system with short-range interactions of remarkable properties. When the scattering length a diverges, $1/ak_F \to 0$ (k_F is the Fermi momentum of the system), the low-energy s-wave scattering phase shift is $\delta_0 = \pi/2$. The ground state energy per particle E_0 is proportional to the one of the noninteracting Fermi gas E_{FG} in a box:

$$E_0 = \xi E_{FG} = \xi \frac{3}{10}\frac{\hbar^2 k_F^2}{M}, \tag{1}$$

where the constant ξ is known as the Bertsch parameter and M is the mass of the fermion. In the limit $ak_F \to -\infty$, quantum Monte Carlo (QMC) results give the exact value of $\xi = 0.372(5)$ [2], in agreement with experiments [3, 4].

One signature of superfluidity is the formation of quantized vortices. Since their first observations in superfluid ^{4}He a large body of experimental and theoretical work has been carried out concerning bosonic systems [5–8]. On the other hand, the discovery of vortex lattices in a strongly interacting rotating Fermi gas of ^{6}Li [9] was a milestone in the study of superfluidity in cold Fermi gases.

A vortex line consists of an extended irrotational flow field, with a core region where the vorticity is concentrated. The quantization of the flow manifests itself in the quantized units $h/2M$ of circulation. There is no evidence for quantized vortices with more than one unit of circulation. Many questions remain to be answered concerning the structure of the vortex core for fermions.

In this paper we focus on ultracold Fermi gases, but our results are useful to also understand properties of related systems. Ultracold atomic gases and low-density neutron matter are unique in the sense that both exhibit pairing gaps of the order of the Fermi energy [10]. The neutron scattering length is about -18.5 fm which is significantly larger than the interparticle spacing and the interaction range 2.7 fm [11], therefore low density neutron matter is also near unitarity. In this regime both dilute cold fermion atoms and neutron matter have similar properties [12]. The possibility of tuning particle-particle interactions experimentally in cold atomic gases provides an emulation of low-density neutron matter, which is beyond direct experimental reach. We present results of the vortex structure in cold atomic gases, that can be extended to direct simulations of vortices in superfluid neutron matter using realistic nuclear Hamiltonians.

Here we report results for a single vortex line in the unitary Fermi gas in a cylindrical geometry. We found that the density profile is flat at the center of the cylinder. We separated from the ground state of the system the wall contribution, and determined an upper bound of the bulk energy as $E_0 = (0.50 \pm 0.01)E_{FG}$ per particle. E_{FG} is the free Fermi gas energy at the same geometry, defined as

$$E_{FG} = \frac{3}{10}\frac{\hbar^2}{M}\left(3\pi^2\frac{A}{V}\right)^{2/3}, \tag{2}$$

where A is the number of particles, and V is the volume. We also estimated an upperbound value of the superfluid pairing gap for this geometry, $\Delta = (1.12 \pm 0.02)E_{FG}$. For the system with a vortex line we obtained the density profile with a non-zero density at the core, and an excitation energy of $E_{ex} = (8.6 \pm 0.3)10^{-3}E_{FG}$ per particle.

We have organized this work as follows. In Section II we present the methods employed to treat our system. We begin with the solution of Schroedinger's equation for a spinless free-particle in a cylindrical container. In Section II B we show that the component of the BCS wave function with a fixed number of particles can be written

* lucas.madeira@asu.edu

as an antisymmetrized product of pairing functions, determined for the cylindrical geometry. We introduce the ground state wave function and the wave function for the system with a vortex line in Sections II C and II D, respectively. The QMC methods we employed are briefly described in Section II E. Section III contains our results. First we present the spatial distribution of the particles in the cylinder for both the ground state and the system with a vortex line. Energy related quantities, such as the ground state energy, the superfluid pairing gap and the vortex excitation energy are given in Sec. III B. Finally, we discuss our results in Section IV.

II. METHODS

Previous calculations on Bose systems like ^{4}He have often used a periodic array of counter rotating vortices in order to have periodic boundary conditions to minimize surface effects. For example, in ^{4}He the calculations of Ref. 13 used 300 particles and 4 counter rotating vortices in the simulation cell. In order to use the same number of fermion pairs we would require a system of 600 fermions. While a few simulations of fermions have been performed with this number of particles, the required variance for a detailed optimization is beyond the goals of this paper. We used a circular cylindrical simulation cell of radius $\mathcal{R}$ with hard wall boundary conditions, at this radius. The system is periodic in the axial direction.

We begin our calculations by investigating properties of the ground state of the system. The model we considered consists of A spin-1/2 fermions in a cylinder of radius $\mathcal{R}$ and height $\mathcal{L}$. Because the system is dilute, the interaction is s-wave. Fermions of the same spin do not interact and we use a short range potential that is attractive, which can reproduce the regime of $ak_F \to -\infty$. The s-wave potential $V(r)$ acting between particles with opposite spin has the form

$$V(r) = -v_0 \frac{2\hbar^2}{M} \frac{\mu^2}{\cosh^2(\mu r)}, \tag{3}$$

where v_0 can be adjusted to tune the value of ak_F and μ controls the effective range r_{eff} of the potential. We set $v_0 = 1$ that for this potential correspond to $a = \pm\infty$ and $r_{eff} = 2/\mu$ [14, 15]. In this paper all the calculations are performed with $\mu r_0 = 24$, and $4\pi r_0^3 n_0 = 3$, where n_0 is the number density, but the results could be straightforwardly extrapolated as done in Ref. 16.

A. Schroedinger's equation in cylindrical coordinates

We considered the free particle solution of Schroedinger's equation in a cylinder of radius $\mathcal{R}$ and height $\mathcal{L}$, finite at $\rho = 0$ and subject to the boundary conditions

$$\begin{aligned} \Psi_{nmp}(\rho = \mathcal{R}, \varphi, z) &= 0, \\ \Psi_{nmp}(\rho, \varphi, z) &= \Psi_{nmp}(\rho, \varphi + 2\pi, z), \\ \Psi_{nmp}(\rho, \varphi, z) &= \Psi_{nmp}(\rho, \varphi, z + \mathcal{L}), \end{aligned} \tag{4}$$

where (ρ, φ, z) are the usual cylindrical coordinates. The solution is given by

$$\Psi_{nmp}(\rho, \varphi, z) = \mathcal{N}_{mp} J_m(k_{mp}\rho) \exp[i(k_z z + m\varphi)], \tag{5}$$

where $\mathcal{N}_{mp}$ is a normalization constant, $J_m(k_{mp}\rho)$ are Bessel functions of first-kind, $k_{mp} = j_{mp}/\mathcal{R}$, j_{mp} is the p-th zero of J_m, and $k_z = 2\pi n/\mathcal{L}$. The quantum numbers n and m can take the values $0, \pm1, \pm2, \ldots$ and $p = 1, 2, \ldots$. The eigenvalues of these functions are

$$E_{nmp} = \frac{\hbar^2}{2M} \left[\left(\frac{j_{mp}}{\mathcal{R}} \right)^2 + \left(\frac{2\pi n}{\mathcal{L}} \right)^2 \right]. \tag{6}$$

The set of states $\{\Psi_{nmp}\}$ is complete, therefore it is used to expand our many-body trial wave function.

B. BCS wave function projected to a fixed number of particles

The BCS wave function used to describe the Cooper pairs in the ground state, is written as

$$\begin{aligned} |BCS\rangle_\theta &= \prod_{\mathbf{k}} (u_{\mathbf{k}} + e^{i\theta} v_{\mathbf{k}} \hat{a}^\dagger_{\mathbf{k}\uparrow} \hat{a}^\dagger_{-\mathbf{k}\downarrow}) |0\rangle, \\ u_{\mathbf{k}}^2 + v_{\mathbf{k}}^2 &= 1, \end{aligned} \tag{7}$$

where $u_{\mathbf{k}}$ and $v_{\mathbf{k}}$ are real numbers, θ is a phase, $\mathbf{k}$ is the wave number vector, $\hat{a}^\dagger_{\mathbf{k}\uparrow(\downarrow)}$ creates a fermion with momentum $\mathbf{k}$ and spin up (down), and $|0\rangle$ represents the vacuum. However this function is not an eigenstate of the particle number operator. The BCS wave function projected to a fixed number A of particles, half of them with spin up and the other half with spin down, can be written as the antisymmetrized product [17]

$$\begin{aligned} \psi_{BCS}(\mathbf{R}, S) = \mathcal{A}[&\phi(\mathbf{r}_1, s_1, \mathbf{r}_2, s_2) \times \\ &\times \phi(\mathbf{r}_3, s_3, \mathbf{r}_4, s_4) \ldots \phi(\mathbf{r}_{A-1}, s_{A-1}, \mathbf{r}_A, s_A)], \end{aligned} \tag{8}$$

where $\mathbf{R}$ is a vector containing the particle positions $\mathbf{r}_i$, S stands for the spins s_i and ϕ is the pairing function. This wave function can be calculated efficiently as a Slater determinant or a pfaffian [18]. The simulation is performed by using pairing orbitals constructed from the functions of Eq. 5, instead of plane waves typically employed in a periodic box or in an harmonic trap [19]. The pairing orbitals are given by

$$\begin{aligned} &\phi(\mathbf{r}_1, s_1, \mathbf{r}_2, s_2) = \sum_{\mathbf{k}} \frac{v_{\mathbf{k}}}{u_{\mathbf{k}}} \mathcal{N}_{mp}^2 J_m\left(\frac{j_{mp}\rho_1}{\mathcal{R}} \right) \times \\ &J_m\left(\frac{j_{mp}\rho_2}{\mathcal{R}} \right) \exp\{i[k_z(z_1 - z_2) + m(\varphi_1 - \varphi_2)]\} \times \\ &[\langle s_1 s_2| \uparrow\downarrow\rangle - \langle s_1 s_2| \downarrow\uparrow\rangle], \end{aligned} \tag{9}$$

where we have explicit included the spin part to impose singlet pairing.

We also want to simulate systems that are not fully paired, by including unpaired states using a superposition of free-particle solutions

$$\Phi(\rho,\varphi,z)=\sum_{n,m,p}\nu_{nmp}\Psi_{nmp}(\rho,\varphi,z), \tag{10}$$

where the ν_{nmp} are variational parameters. For q pairs and o unpaired states, $A=2q+o$, we have

$$\begin{aligned}&\psi_{BCS}(\mathbf{R},S)=\\&\mathcal{A}[\phi(\mathbf{r}_1,s_1,\mathbf{r}_2,s_2)\dots\phi(\mathbf{r}_{2q-1},s_{2q-1},\mathbf{r}_{2q},s_{2q})\times\\&\Phi_{2q+1}(\mathbf{r}_{2q+1})\dots\Phi_{2q+o}(\mathbf{r}_{2q+o})].\end{aligned} \tag{11}$$

as described in Ref. [14].

C. Ground state

For the ground state of fermions in a cylindrical container, we use Eq. (8), or Eq. (11) if we have unpaired particles. The momentum vectors in the cylinder are quantized and the system has a shell structure that depends on $\mathcal{R}$ and $\mathcal{L}$, see Eq. (6). We consider $\alpha_{\mathbf{k}}\equiv v_{\mathbf{k}}/u_{\mathbf{k}}$ as variational parameters [20] and we assume the pairing wave functions to be

$$\begin{aligned}\phi(\mathbf{r},\mathbf{r}')=\tilde{\beta}(\mathbf{r},\mathbf{r}')+\sum_{I\leqslant I_C}\alpha_I\mathcal{N}_{mp}^2J_m\left(\frac{j_{mp}\rho}{\mathcal{R}}\right)\times\\ J_m\left(\frac{j_{mp}\rho'}{\mathcal{R}}\right)\exp\left\{i\left[k_z(z-z')+m(\varphi-\varphi')\right]\right\},\end{aligned} \tag{12}$$

where we adopted hereafter primed indexes to denote spin-down particles, unprimed ones to refer to spin-up particles and we omit the spin part. In Eq. (12), I_C is a cutoff shell number and we assume that contributions of shells with $I>I_C$ are included through the $\tilde{\beta}(\mathbf{r},\mathbf{r}')$ function, given by

$$\tilde{\beta}(\mathbf{r},\mathbf{r}')=\begin{cases}\mathcal{N}_{01}^2J_0\left(\frac{j_{01}\rho}{\mathcal{R}}\right)J_0\left(\frac{j_{01}\rho'}{\mathcal{R}}\right)\times\\ \times\beta(r)+\beta(\mathcal{L}-r)-2\beta(\mathcal{L}/2) & \text{for } r\leqslant\mathcal{L}/2\\ 0 & \text{for } r>\mathcal{L}/2\end{cases}$$

and

$$\beta(r)=[1+\gamma br][1-e^{-cbr}]\frac{e^{-br}}{cbr}, \tag{13}$$

where $r=|\mathbf{r}-\mathbf{r}'|$ and b, c and γ are variational parameters. This functional form of $\beta(r)$ describes the short-distance correlation of particles with anti-parallel spins. We consider $c=10$, $\gamma=5$ and $b=0.5\ k_F$.

We also include a one-body Jastrow factor of the form

$$\chi(\rho_i)=\left(\frac{a}{\sqrt{2\pi\sigma^2}}\exp\left\{\frac{(\rho_i-\bar{\rho})^2}{2\sigma^2}\right\}+\nu\right)^{\lambda}, \tag{14}$$

where a, σ, $\bar{\rho}$, ν and λ are variational parameters. The correlation between antiparallel spins is included in the two-body Jastrow factor $f(r_{ij'})$ obtained from solutions of the two-body Schroedinger equation

$$\left[-\frac{1}{M}\nabla^2+V(r)\right]f(r<d)=\lambda f(r<d), \tag{15}$$

where d is a variational parameter. The boundary conditions are $f(r>d)=1$ and $f'(r=d)=0$ [21]. The total wave function for the ground state of fermions in a cylindrical container is then written as

$$\psi_0(\mathbf{R})=\prod_k\chi(\rho_k)\prod_{i,j'}f(r_{ij'})\psi_{BCS}(\mathbf{R}). \tag{16}$$

D. Vortex line

The simulation of a vortex excitation is done by considering pairing orbitals that are eigenstates of L_z with eigenvalues $\pm\hbar$. This is done by coupling single particle states of quantum numbers m and $(-m+1)$. In this case we consider pairing orbitals with of form

$$\begin{aligned}\phi_V(\mathbf{r},\mathbf{r}')=\tilde{\beta}(\mathbf{r},\mathbf{r}')+\sum_{i=1}^{K}\tilde{\alpha}_i\mathcal{N}_{m;p}\mathcal{N}_{-m+1;p}\,\{\\ J_m\left(\frac{j_{mp}\rho}{\mathcal{R}}\right)J_{-m+1}\left(\frac{j_{-m+1;p}\rho'}{\mathcal{R}}\right)\times\\ \exp\left\{i\left[k_z(z-z')+m\varphi+(-m+1)\varphi')\right]\right\}+\\ J_m\left(\frac{j_{mp}\rho'}{\mathcal{R}}\right)J_{-m+1}\left(\frac{j_{-m+1;p}\rho}{\mathcal{R}}\right)\times\\ \exp\left\{i\left[k_z(z'-z)+m\varphi'+(-m+1)\varphi)\right]\right\}\},\end{aligned} \tag{17}$$

where K is the number of single particle states with quantum numbers (n,m,p) being paired with $(-n,-m+1,p)$. Since we don't want to have a winding number in the z direction, we consider the quantum number n for a particle and the time-reversed $-n$ for the other. Also, the largest contribution is assumed to be from states with the same quantum number p in the radial part.

E. Diffusion Monte Carlo

The Hamiltonian of our system is given by

$$H=-\frac{\hbar^2}{2M}\sum_i\nabla_i^2+\sum_{i<j}V(r_{ij})\,. \tag{18}$$

The diffusion Monte Carlo method (DMC) is used to extract the lowest energy state of H from an initial state ψ_T obtained through Variational Monte Carlo (VMC) calculations. The propagation of the system in an imaginary time τ can formally be written as

$$\psi(\tau)=e^{-(H-E_T)\tau}\psi_T, \tag{19}$$

where we introduce an energy offset E_T, used to control the normalization of $\psi(\tau)$. In the limit $\tau \to \infty$, only the lowest energy component Φ_0, not orthogonal to ψ_T, survives

$$\lim_{\tau\to\infty} \psi(\tau) = \lim_{\tau\to\infty} e^{-(H-E_T)\tau}\psi_T = \Phi_0. \quad (20)$$

The evolution in imaginary time is performed by solving the integral equation

$$\psi(\mathbf{R},\tau) = \int d\mathbf{R}' G(\mathbf{R},\mathbf{R}',\tau)\psi_T(\mathbf{R}'), \quad (21)$$

where $G(\mathbf{R},\mathbf{R}',\tau)$ is the Green's function of the Hamiltonian, which contains a diffusion term, related to the kinetic operator, and a branching term depending on the potential. The exact form of $G(\mathbf{R},\mathbf{R}',\tau)$ is known only for very simple cases, but it can be approximated in the limit of $\Delta\tau \to 0$. An importance sampled version of Eq. (21) is then solved iteratively with small time step, for a large number of steps. The DMC method can only sample positive distributions. A system formed by fermions has the so-called fermion sign problem. We overcome this problem by using the usual fixed-node approximation [22]. For a detailed description of the DMC algorithm, the importance sample technique and the fermion sign problem, the reader is referred to the review Ref. 23 and references therein.

Note that the trial wave function $\Psi_T(\mathbf{R})$ is used in two different ways: as an approximation of the ground state in the VMC calculation and as importance function that also determines the nodal surface followed by the fixed-node approximation.

The variational parameters for the pairing functions and two-body Jastrow factor have been optimized using the stochastic reconfiguration method [24]. The parameters for the one-body term are chosen to maximize the overlap of the density profile along the radial coordinate calculated using DMC and VMC.

III. RESULTS

In this section we present the results obtained with the BCS wave function ψ_0 for fermions in a cylinder, Eq. (16); and the results for the system with a vortex line along the z-axis, ψ_V using the pair orbitals of Eq. (17). Expectation values of operators that do not commute with the Hamiltonian, such as the density, can be calculated using a combination of mixed and variational estimators,

$$\langle\Phi|\hat{S}|\Phi\rangle \approx 2\langle\Phi|\hat{S}|\Psi_T\rangle - \langle\Psi_T|\hat{S}|\Psi_T\rangle + \mathcal{O}\left[(\Phi-\Psi_T)^2\right]. \quad (22)$$

Such combinations of VMC and DMC estimators are called extrapolated estimators [25].

We have fixed the number density at $k_F^3/(3\pi^2)$, which is the density of the free Fermi gas and we have freedom to choose the radius $\mathcal{R}$ and the height $\mathcal{L}$ of the cylinder. In most simulations we set $\mathcal{L} = 2\mathcal{R}$, so that the diameter is equal to the height of the cylinder; we have verified that this last choice does not affect the results.

A. Density profile

The spatial distribution of the particles in the cylinder was studied by calculating the density profile $\mathcal{D}(\rho)$ along the radial direction ρ. The normalization is chosen so that

$$\int_V \mathcal{D}(\rho)dv = 1, \quad (23)$$

where the integral is over the volume $V = \pi\mathcal{R}^2\mathcal{L}$ of the cylinder.

The ground state density profile for closed shells of the system is presented in Fig. 1. Boundary effects decrease as the number of particles considered is increased. For the largest system the density has small fluctuations near the center of the cylinder and it smoothly decreases until it vanishes at the wall. The almost constant density for small ρ is consistent with the ground state, since it corresponds to the bulk of the system. For the largest number of particles we have considered we assume size effects to be negligible.

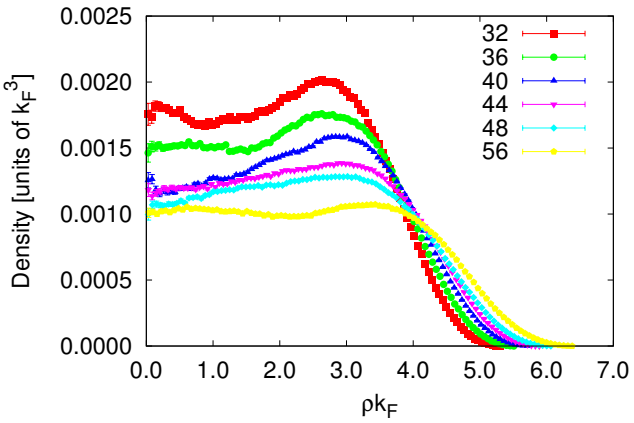

FIG. 1. (Color online) Ground state density profile for systems with closed shells, corresponding to different number of particles as indicated in the legend.

We present the density profile for closed shell systems with a vortex line excitation in Fig. 2. The most interesting feature of this quantity is a non-zero density at the core, near $\rho = 0$. Previous calculations using Bogoliubov-deGennes theory[26, 27] while showing a finite density at the origin, give a much larger suppression of the density at the origin. Their density at the origin and unitarity is about one quarter of the bulk density. We do not see such a large suppression. The reasons for these differences could be due to our geometry, the fixed-node approximation we use, or the approximations in the

Bogoliubox-deGennes theory. Future calculations using both methods in the same geometry could help shed light on these differences.

We calculated the particle number a distance R from the cylinder axis as

$$\eta(R) = \int_0^L dz \int_0^{2\pi} d\varphi \int_0^R d\rho\ \rho\ \mathcal{D}(\rho). \qquad (24)$$

We find that the difference between $\eta(R)$ for the ground state and the vortex line state is at most 2 particles. The optimization process is computationally costly and it may be responsible for the difficulties in resolving the densities of the two systems.

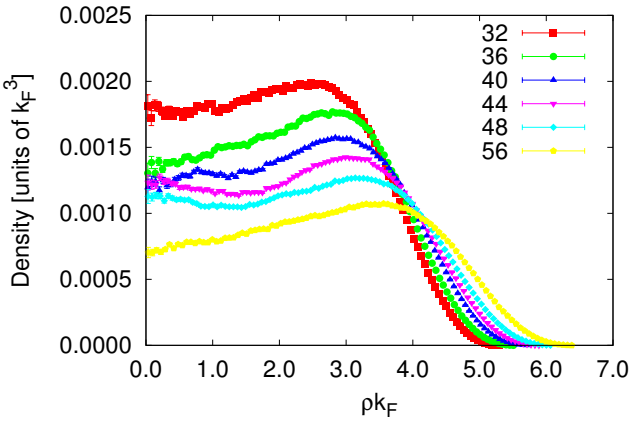

FIG. 2. (Color online) Density profile for systems with a vortex line and closed shells for different number of particles.

B. Energy

1. *Ground state*

The energy per particle of the system in the cylindrical geometry goes to the value of the bulk energy per particle in the limit of $\mathcal{R}, \mathcal{L} \to \infty$. Since the wave function vanishes at the cylinder walls of our finite system, the energy has a dependence on the surface area of the wall, $S = 2\pi\mathcal{R}\mathcal{L} = 4\pi\mathcal{R}^2$. However, we still are able to estimate the bulk energy. We extrapolate the energy per particle as a function of the radius using the functional form

$$E(\mathcal{R}) = \frac{E(\mathcal{R})}{A} = E_0 + \frac{E_s}{4\pi\mathcal{R}^2}, \qquad (25)$$

where E_0 and E_s are constants, that represent the bulk and surface energies. The resulting parameters are $E_0 = (0.50 \pm 0.01)E_{FG}$ and $E_s = (55.2 \pm 1.0)E_{FG}k_F^{-2}$, and $E(\mathcal{R})$ is shown in Fig. 3. The E_0 parameter in this geometry is analogous to the Bertsch parameter in the box with periodic boundary conditions. The energy levels are much more degenerate in the box if compared to the cylinder. The translational invariance gives a good basis for plane waves, while Bessel functions are not as well defined for the radial direction, which leads to a trial function with more parameters needed to simulate systems with the same number of particles. For example, early QMC calculations in the box [14] obtained an upper bound of the Bertsch parameter $\xi = 0.440(2)$ for $A = 38$ using 5 parameters analogous to the α_I of Eq. (12), so that the highest energy single particle state has $k^2_{\rm max} \approx 1.46\ k_F^2$. If we consider the same number of particles and number density in the cylindrical geometry, we require 12 α_I to reach the same $k^2_{\rm max}$. This increased degeneracy may account for the higher values of E_0 when compared to the upper bound of the Bertsch parameter $\xi = 0.383(1)$ [28, 29] and its exact value[2], $\xi = 0.372(5)$.

These differences between the periodic box simulations and the cylindrical simulations show that the calculated properties are significantly biased by the geometry. The clear dependence on system size shown in Fig. 3 further indicates that the main cause is due to nodal surface errors in our fixed-node calculations.

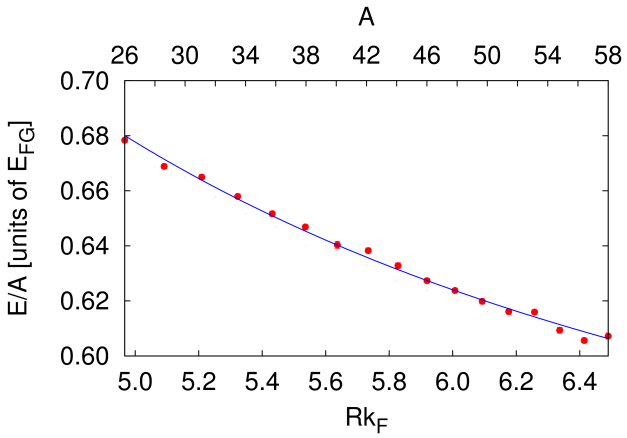

FIG. 3. (Color online) Ground state energy per particle for different system sizes. The solid line corresponds to the energy per particle as a function of $\mathcal{R}$, Eq. (25).

We performed one simulation doubling the height of the cylinder and the number of particles we have used in our calculation with $A = 26$. The energy per particle for this system is $(0.683 \pm 0.001)E_{FG}$, which differs less than 1% from the value found for $A = 26$, $(0.678 \pm 0.001)E_{FG}$, verifying that our results are independent of the condition $\mathcal{L} = 2\mathcal{R}$.

2. *Superfluid pairing gap*

Experiments with cold atom gases determined the pairing gap to be approximately half of the Fermi energy [30, 31]. The pairing gap at $T = 0$ is calculated using the

odd-even staggering formula [10]

$$\Delta(A+1) = E(A+1) - \frac{1}{2}\left[E(A) + E(A+2)\right]. \quad (26)$$

We consider that, for an even number of particles, all of them are paired. For a system with an odd number of particles, the unpaired particle is described by Eq. (10), and we take the coefficients ν_{nmp} as variational parameters. We assume that n and m are good quantum numbers for the unpaired particle, because we employ periodic boundary conditions in the z-direction and the wave function must be an eigenstate of L_z. Thus, we chose the wave function of the unpaired particle to be a linear combination of free particle states with same n and m, but different p, hence Eq. (10) reduces to a sum only over p. We perform independent simulations for different values of n and m and we determine the $\{\nu_{nmp}\}$ which minimize the total energy of the system. In the calculation of the gap we choose the unpaired orbital that gives the lowest energy. This is analogous to previous calculations in the bulk [15, 32]. In Fig. 4 we show the total energy of the system for $26 \leqslant A \leqslant 58$. The pairing gap is estimated through Eq. (26), $\Delta = (1.12 \pm 0.02)E_{FG}$. It is noteworthy that the pairing gap is calculated using the difference of energy upper bounds, thus the result is sensitive to the relative quality of the nodal structure. It is likely that the optimization of the excited state wave function is less effective, which would overestimate the pairing gap. We also note that finite size effects might be canceled out in this calculation that does not consider the vortex line.

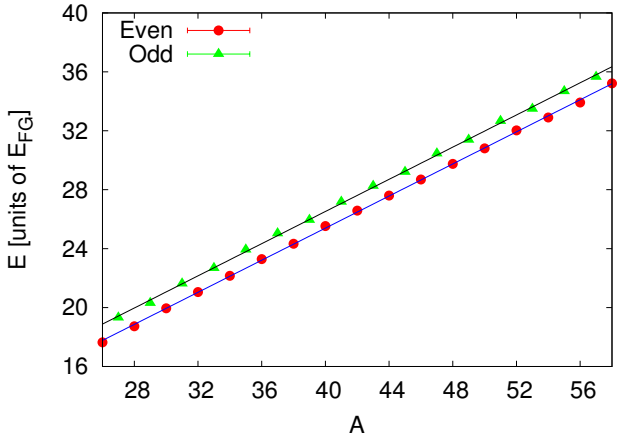

FIG. 4. (Color online) Ground state energy for even (circles) and odd (triangles) number of particles. The solid lines correspond to linear fits of the energy as a function of the number of particles for systems with even and odd number of particles.

3. *Excitation energy*

The excitation energy for a system with a vortex line in our geometry is given by the difference between the energies of the excited state and the ground state. In Fig. 5 we present the excitation energy, as well as the ground state and system with a vortex line energies, for $26 \leqslant A \leqslant 58$. The average of the excitation energies per particle in our geometry for the larger systems ($42 \leqslant A \leqslant 58$) is $E_{ex} = (1.03 \pm 0.04)10^{-2}E_{FG}$.

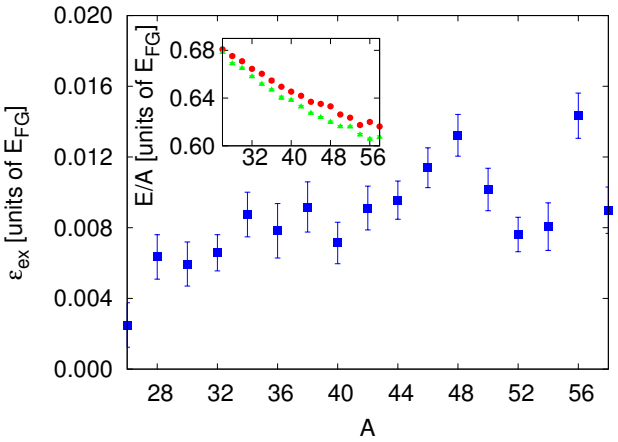

FIG. 5. (Color online) Excitation energy per particle. The inset shows the ground state energies (triangles) and the energy of the system with a vortex line (circles).

IV. DISCUSSIONS AND CONCLUSIONS

In this work, we have calculated the density profiles of the ground state and an excited state with a vortex line for a system of ultracold fermionic atoms at unitarity. For systems with $A \geqslant 36$ the ground state density profiles are flat near the center of the cylinder and they smoothly decrease until the density vanishes at the wall. The most interesting feature of the density profile of the systems with a vortex line is a non-vanishing density at the core, $\rho = 0$. However, it is lower than the ground state density by a small amount. Since the Cooper pairs have non-zero size, it is possible for a pair to have non-zero angular momentum at the origin and still have a non-zero density there.

For the cylindrical geometry, we calculated the energy of the ground state for an even number of particles (all paired). Because the wave function vanishes at the walls of the cylinder, we need very large values of $\mathcal{R}$ and $\mathcal{L}$ to neglect the effects introduced by this condition. We proposed a functional form for the energy per particle as a function of the radius of the cylinder which takes into account the energy term due to the walls.

The superfluid pairing gap of these ultracold atomic gases is of interest because it is comparable to the Fermi energy of the system. The usual odd-even staggering formula [10] yields a gap of $\Delta = (1.12 \pm 0.02)E_{FG}$. Previous quantum Monte Carlo simulations of fermions in a box, using periodic boundary conditions, predicted

$\Delta = (0.84 \pm 0.05) E_{FG}$ [32]; while an experiment at finite temperature produced the value $\Delta = (0.45 \pm 0.05) E_{FG}$ [31].

Future calculations will include more detailed study of the vortex structure, the excitations of the fluid in the presence of the vortex, and calculations of the reduced density matrices in order to better understand the condensate in the presence of vortices.

We developed a wave function to study superfluidity and vortices in a cylindrical geometry. This geometry enabled us to simulate a vortex line in a superfluid Fermi gas using a bare Hamiltonian. These calculations allowed theoretical predictions of the structure of vortices that can be compared with experiments. Our results have implications both for cold atom research and for astrophysics where the vortex structure in the superfluid crust of neutron stars is not well understood. This work can be extended to study vortices in superfluid neutron matter by extending the calculations of Ref. 18 and 33.

ACKNOWLEDGMENTS

This work was partially supported by grants 10/10072-0, 12/24195-2, 13/19853-3 and 14/20864-2 from FAPESP and 087/2012 PVE/CAPES. The work of S.G. is supported by the U.S. Department of Energy, Office of Nuclear Physics, under contracts DE-AC52-06NA25396, and by the NUCLEI SciDAC program. K.S. was partially supported by the National Science Foundation grant PHY-1404405. Computational resources have been provided by Los Alamos Open Supercomputing and CENAPAD-SP at Unicamp. We also used resources provided by NERSC, which is supported by the US DOE under Contract DE-AC02-05CH11231.

[1] C. A. Regal, M. Greiner, and D. S. Jin, Phys. Rev. Lett. **92**, 040403 (2004).
[2] J. Carlson, S. Gandolfi, K. E. Schmidt, and S. Zhang, Phys. Rev. A **84**, 061602 (2011).
[3] M. J. H. Ku, A. T. Sommer, L. W. Cheuk, and M. W. Zwierlein, Science **335**, 563 (2012).
[4] G. Zürn, T. Lompe, A. N. Wenz, S. Jochim, P. S. Julienne, and J. M. Hutson, Phys. Rev. Lett. **110**, 135301 (2013).
[5] R. Donnelly, *Quantized Vortices in Helium II*, Cambridge Studies in American Literature and Culture No. v. 2 (Cambridge University Press, 1991).
[6] S. A. Vitiello, L. Reatto, G. V. Chester, and M. H. Kalos, Phys. Rev. B **54**, 1205 (1996).
[7] G. Ortiz and D. M. Ceperley, Phys. Rev. Lett. **75**, 4642 (1995).
[8] S. Giorgini, J. Boronat, and J. Casulleras, Phys. Rev. Lett. **77**, 2754 (1996).
[9] M. W. Zwierlein, J. R. Abo-Shaeer, A. Schirotzek, C. H. Schunck, and W. Ketterle, Nature **435**, 1047 (2005).
[10] J. Carlson, S. Gandolfi, and A. Gezerlis, *Fifty Years of Nuclear BCS*, edited by R. A. Broglia and V. Zelevinsky (World Scientific Publishing Company, 2013).
[11] A. Gezerlis and J. Carlson, Phys. Rev. C **77**, 032801(R) (2008).
[12] J. Carlson, S. Gandolfi, and A. Gezerlis, PTEP **2012**, 01A209 (2012).
[13] M. Sadd, G. V. Chester, and L. Reatto, Phys. Rev. Lett. **79**, 2490 (1997).
[14] J. Carlson, S.-Y. Chang, V. R. Pandharipande, and K. E. Schmidt, Phys. Rev. Lett. **91**, 050401 (2003).
[15] S. Y. Chang, V. R. Pandharipande, J. Carlson, and K. E. Schmidt, Phys. Rev. A **70**, 043602 (2004).
[16] M. M. Forbes, S. Gandolfi, and A. Gezerlis, Phys. Rev. A **86**, 053603 (2012).
[17] Bouchaud, J.P., Georges, A., and Lhuillier, C., J. Phys. France **49**, 553 (1988).
[18] S. Gandolfi, A. Y. Illarionov, F. Pederiva, K. E. Schmidt, and S. Fantoni, Phys. Rev. C **80**, 045802 (2009).
[19] J. Carlson and S. Gandolfi, Phys. Rev. A **90**, 011601 (2014).
[20] See Supplemental Material at http://fermi.la.asu.edu/vortex/tables.pdf,for the variational parameters of Equations 10, 12, 14 and 17 for the different system sizes.
[21] S. Cowell, H. Heiselberg, I. E. Mazets, J. Morales, V. R. Pandharipande, and C. J. Pethick, Phys. Rev. Lett. **88**, 210403 (2002).
[22] J. B. Anderson, The Journal of Chemical Physics **63**, 1499 (1975).
[23] W. M. C. Foulkes, L. Mitas, R. J. Needs, and G. Rajagopal, Rev. Mod. Phys. **73**, 33 (2001).
[24] M. Casula, C. Attaccalite, and S. Sorella, The Journal of Chemical Physics **121**, 7110 (2004).
[25] D. Ceperley and H. Kalos, *Monte Carlo Methods in Statistics Physics Quantum Many-Body Problems*, edited by K. E. Binder, Vol. 7 (Springer-Verlag, 1986).
[26] A. Bulgac and Y. Yu, Phys. Rev. Lett. **91**, 190404 (2003).
[27] R. Sensarma, M. Randeria, and T.-L. Ho, Phys. Rev. Lett. **96**, 090403 (2006).
[28] S. Gandolfi, K. E. Schmidt, and J. Carlson, Phys. Rev. A **83**, 041601 (2011).
[29] M. M. Forbes, S. Gandolfi, and A. Gezerlis, Phys. Rev. Lett. **106**, 235303 (2011).
[30] Y. Shin, C. H. Schunck, A. Schirotzek, and W. Ketterle, Phys. Rev. Lett. **99**, 090403 (2007).
[31] J. Carlson and S. Reddy, Phys. Rev. Lett. **100**, 150403 (2008).
[32] J. Carlson and S. Reddy, Phys. Rev. Lett. **95**, 060401 (2005).
[33] S. Gandolfi, A. Y. Illarionov, S. Fantoni, F. Pederiva, and K. E. Schmidt, Phys. Rev. Lett. **101**, 132501 (2008).